

The crystal structure of gearsutite, $\text{CaAlF}_4(\text{OH})\cdot\text{H}_2\text{O}$

FABIO MARCHETTI^{1,*} AND NATALE PERCHIAZZI²

¹DIPARTIMENTO DI INGEGNERIA CHIMICA, DEI MATERIALI DELLE MATERIE PRIME E METALLURGIA, UNIVERSITÀ DEGLI STUDI DI ROMA "LA SAPIENZA,"
VIA DEL CASTRO LAURENZIANO, 7, I-00195 ROMA, ITALY

²DIPARTIMENTO DI SCIENZE DELLA TERRA, UNIVERSITÀ DI PISA, VIA S. MARIA, 53, 56126 PISA, ITALY

ABSTRACT

The discovery of unusually well-crystallized samples of gearsutite allowed determination of its crystal structure. The crystals belong to space group $P1$, $a = 4.940(1)$, $b = 6.810(1)$, $c = 6.978(1)$ Å; $\alpha = 101.12(1)$, $\beta = 94.86(1)$, $\gamma = 110.07(1)^\circ$; $V = 213.43(6)$ Å³; $Z = 2$. The structure consists of layers of eightfold-coordinated calcium polyhedra connected through pairs of $[\text{Al}_2\text{F}_8(\text{OH})_2]$ octahedra which are oriented identically, similar to those observed in other hydroxyl aluminum fluorides. A comparison with other minerals of similar composition is made. The structure data allowed us to reliably index the powder pattern and to show that the reflection intensities are strongly affected by preferred orientation.

INTRODUCTION

Gearsutite, $\text{CaAlF}_4(\text{OH})\cdot\text{H}_2\text{O}$, was discovered by Hagemann (in Dana 1868) in the cryolite deposit of Ivigtut, Greenland. It has subsequently been found, as a late stage mineral in a wide variety of environments all over the world, commonly in white earthy masses. At the La Veneziana mine, Veneto, Italy (Boscardin et al. 1995), it is found as a secondary mineral, associated with Cu-alteration minerals such as ramsbeckite and posnjakite. At Vulcano island, Sicily, Italy, it is found as a fumarolic phase (Bernauer 1941). Raade and Haug (1980) have reported its presence as a late-stage, cavity filling phase in a soda-granite near Oslo, Norway.

Gearsutite crystals generally are small 5–10 µm. The simple composition of gearsutite recalls that of the monoclinic strontium hydroxyfluorides tikhonkovite, $\text{SrAlF}_4(\text{OH})\cdot 2\text{H}_2\text{O}$ (Pudovkina and Pyatenko 1967) and acuminite, $\text{SrAlF}_4(\text{OH})\cdot 2\text{H}_2\text{O}$ (Krogh Andersen and Ploug-Sørensen 1991). However, the generally small size of the crystals, 5–10 µm limit crystallographic study to powder diffraction patterns. Notwithstanding, two different indexing methods suggested the same monoclinic cell with the appropriate volume (427 Å³), we did not succeed in solving the structure by direct methods. Recently, Birch and Pring (1990) reported the presence of an interesting assemblage of fluorine minerals, such as calcium ralstonite, morinite, and gearsutite at the Cleveland mine, Tasmania, Australia. These authors described this mineral assemblage as formed during a hydrothermal low temperature stage of crystallization. They documented the fluorine minerals and especially gearsutite, showed an exceptionally well-developed crystal habit, compared with the normal habit of these minerals. The favorable opportunity stimulated us to undertake a single crystal study of gearsutite.

This paper also elucidates the relationships of gearsutite with other fluorides and correctly indexes its powder pattern.

STRUCTURE DETERMINATION

A colorless platy crystal fragment of gearsutite from the Cleveland Mine (Tasmania) was used for intensity data collection, performed on a Siemens P4 diffractometer. Table 1 summarizes the intensity data collection and of the crystal structure refinement.

The cell parameters were obtained by least squares fitting of 29 reflections with 2θ in the range 21–28°. The collected intensities were corrected for Lorentz and polarization effects and for absorption by means of a semiempirical method based on ψ scans. The structure was solved by direct methods (SHELXTL: Sheldrick 1992) and completed by standard Fourier procedure. The positions of the hydrogen atoms were located on the difference Fourier map and were not refined. In the last refinement cycles anisotropic displacements parameters were refined for all the non hydrogen atoms and the reliability factors listed in Table 1 were obtained. Final positional coordinates and equivalent isotropic thermal parameters B_{eq} are reported in Table 2.

Further details of the crystal structure determination in the form of CIF files have been deposited with FACHINFORMATIONSZENTRUM KARLSRUHE, D-76344 Eggenstein-Leopoldshafen (Germany), under the depository number CSD-410611. The relevant bond lengths and angles are collected in Table 3.

DESCRIPTION OF THE STRUCTURE

The crystal structure of gearsutite consists of a network of interconnected $[\text{CaF}_6(\text{OH})_2]$ polyhedra, hereafter CaX_8 , and pairs of $[\text{Al}_2\text{F}_8(\text{OH})_2]$ octahedra, henceforth denoted as Al_2X_{10} . Following the classification of Hawthorne (1984) for aluminofluoride minerals, gearsutite can be classified in the group containing finite clusters, namely the Al_2X_{10} pairs. The coordination geometry of Ca^{2+} , as frequently happens for eightfold coordination,

*E-mail: fama@dcc.unipi.it

TABLE 1. Crystal data and refinement details

Empirical formula	CaAlF ₄ O ₂ H ₃
Formula weight	178.08
Temperature	293(2) K
Wavelength	0.71073 Å
Crystal system, space group	Triclinic, P1
Unit-cell dimensions	a = 4.940(1) Å α = 101.12(1)° b = 6.810(1) Å β = 94.86(1)° c = 6.978(1) Å γ = 110.07(1)°
Volume Z	213.43(6) Å ³
Calculated density	2.2771 Mg/m ³
Absorption coefficient	1.679 mm ⁻¹
F(000)	176
Crystal size	0.085 × 0.14 × 0.03 mm
θ range for data collection	3.02 to 24.99 deg.
Index ranges	-5 ≤ h ≤ 1, -7 ≤ k ≤ 7, -8 ≤ l ≤ 8
Reflections collected / unique	1028 / 748 [R _{int} = 0.0558]
Completeness to 2θ = 24.99	99.7%
Refinement method	Full-matrix least-squares on F ²
Data / restraints / parameters	748 / 0 / 73
Goodness-of-fit* on F ²	1.117
Final R indices* [I > 2σ(I)]	R ₁ = 0.0362, wR ₂ = 0.0731
R indices* (all data)	R ₁ = 0.0545, wR ₂ = 0.0866
Largest diff. peak and hole	0.539 and -0.657 e. Å ⁻³

* Goodness-of-fit = $[\sum [w(F_o^2 - F_c^2)^2] / (N - P)]^{1/2}$, where N, P are the numbers of observations and parameters, respectively, $R_1 = \sum ||F_o| - |F_c|| / \sum |F_o|$; $wR_2 = [\sum [w(F_o^2 - F_c^2)^2] / \sum w(F_o^2)^2]^{1/2}$; $w = 1 / [\sigma^2(F_o^2) + (0.0243Q)^2 + 0.57Q]$ where $Q = [\text{MAX}(F_o^2, 0) + 2F_c^2] / 3$.

TABLE 2. Final atomic coordinates (Å × 10⁴) and displacement parameters (×10³)

	x	y	z	U _{eq} *
Ca	3562(2)	3876(1)	2225(1)	10(1)
Al	-55(3)	8281(2)	3384(2)	8(1)
F1	2315(5)	6851(4)	2942(4)	14(1)
F2	1998(5)	205(4)	2080(4)	13(1)
F3	7342(5)	6746(4)	1146(4)	13(1)
F4	2343(5)	3701(4)	5394(4)	12(1)
OW	7835(7)	2524(5)	1499(5)	15(1)
O1	2202(6)	9948(5)	5884(4)	9(1)

* U_{eq} = $(1/3)\sum_i \sum_j U_{ij} a_i a_j a_i$.

TABLE 3. Main bond distances (Å) in the gearksutite structure

Ca-F3*	2.285(3)	Al-F1	1.773(3)
Ca-F1	2.292(3)	Al-F2§	1.811(3)
Ca-F2	2.328(3)	Al-F3†	1.815(3)
Ca-F3	2.485(3)	Al-F4	1.840(3)
Ca-F4	2.354(3)	Al-O1	1.900(3)
Ca-F4†	2.379(s3)	Al-O1#	1.890(3)
Ca-OW	2.626(3)		
Ca-OW‡	2.626(3)		

Note: Symmetry transformations used to generate equivalent atoms:

* = -x+1, -y+1, -z; || = -x, -y+1, -z+1;
† = -x+1, -y+1, -z+1; # = -x, -y+2, -z+1;
‡ = x-1, y, z; ** = 1-x, -y, -z;
§ = x, y+1, z; †† = 1-x, 2-y, 1-z.

cannot easily be described in terms of an idealized polyhedron. A rational approach to this problem has been suggested by Muettterties and Guggenberger (1973), who proposed comparing a real coordination polyhedron with an idealized one based on dihedral angles between planes defined by the coordinating atoms. Table 4 lists the four δ and the two φ values calculated for the coordination polyhedron of Ca²⁺ in gearksutite together with those of the idealized polyhedral forms with eightfold coordination, namely the dodecahedron (Dod), the bicapped trigonal prism (BTP) and the square antiprism (SAP). Our calcium polyhedron may be described as a bicapped trigonal prism slightly distorted toward the square antiprism.

The calcium polyhedra are interconnected by sharing the two almost opposite edges F3-F3* and F4-F4†, making infinite chains in the c direction (see bottom of Table 3 for the meaning of the

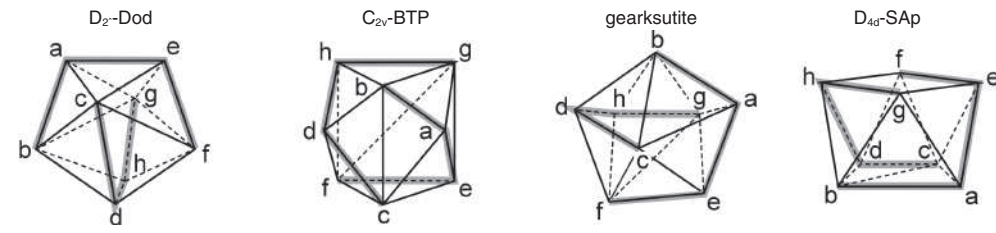
superscripts). Each polyhedron is related to its nearest neighbors by two inversion centers placed in the middle of the shared edges. Similar chains are present in the crystal structure of prosopite, Ca[Al₂F₄(OH)₄] (Giacovazzo and Marchetti 1969).

The two water molecules are placed on opposite apices of the polyhedra (the OW-Ca-OW‡ angle being 140.3°) and the chains are joined by sharing the apices OW. Bidimensionally infinite layers of calcium polyhedra, as those shown in Figure 1, are so built. The layers are puckered and parallel to (010) plane.

Connected chains of nine-coordinated strontium polyhedra are also present in tikhonenkovite, but the sharing is not so extended as in gearksutite, being limited to chain pairs that form "ribbons," indefinitely extending along c.

The aluminum cation is octahedrally coordinated by four fluorines and two hydroxyl groups in the cis position. The octahedra

TABLE 4. Dihedral angles δ and φ suggested by Muettterties and Guggenberger for geometrically defining an eight-coordination polyhedron

	D _{2d} -Dod	C _{2v} -BTP	gearksutite	D _{4d} -SAP
				
δ ₁ a[b, c]d	29.5	21.8	21.7	0
δ ₂ e[c, f]d	29.5	48.2	52.0	52.4
δ ₃ e[g, f]h	29.5	0	10.4	0
δ ₄ a[g, b]h	29.5	48.2	44.3	52.4
φ _A b[a, e]f	0	14.1	19.3	24.5
φ _B c[d, h]g	0	14.1	13.7	24.5

Notes: In gearksutite the labels a, b, c, d, e, f, g, and h correspond to OW‡, F1, F3*, F3, F2, OW, F4, and F4†, respectively. The edges defining φ angles have been reinforced. The f-g and b-c edges in the sketches of Bicapped Trigonal Prism (BTP) and Square Antiprism (SAP), respectively, are not real edges in those polyhedra. (See notes of Table 3.)

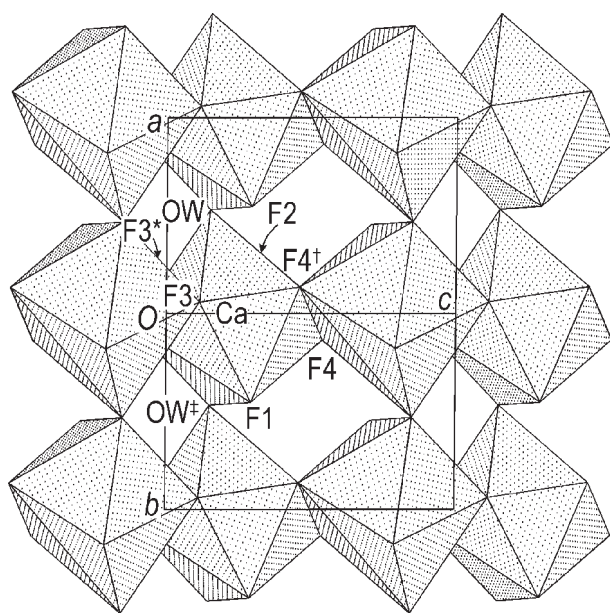


FIGURE 1. Wall of polyhedra $\{CaF_6(OH)_2\}$ projected in the b^* direction.

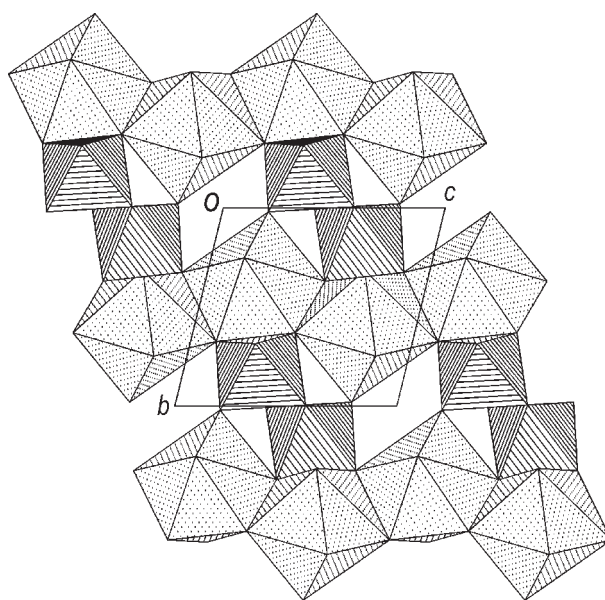


FIGURE 2. The structure of gearksutite projected in the a direction. The aluminum octahedra pairs bridging between the calcium walls can be seen.

of each couple are paired by sharing the OH-OH[†] edge, related by the inversion center placed in the middle of the shared edge. Similar dimers with two bridging OH groups are also found in creedite, $Ca_3Al_2F_8(OH)_2(SO_4) \cdot 2H_2O$ (Giuseppetti and Tadini 1983), acuminite and tikhonenkovite. When both fluorine and OH groups are present around the aluminum, the edge sharing of the two octahedra occurs through the hydroxyl groups, the Al_2X_{10} groups join calcium hydrofluoride layers, by sharing all their eight fluorines with CaX_8 (Fig. 2).

The positions of hydrogen atoms were reliably suggested by the fact that the O1 atom shows only one, whereas OW atom only two, O-O or O-F distances less than 2.9 Å. Moreover, the residual electron density due to the hydrogen atoms was observed in the difference Fourier map between the most likely pairs of anions. The reported hydrogen positions may be taken with reasonable confidence, notwithstanding the low precision of the hydrogen location in X-ray structural analysis. On this basis, we describe a net of hydrogen bonds that contributes to stabilization of the gearksutite structure. The water molecule coordinating the Ca^{2+} ion is engaged as a donor in two hydrogen bonds with O1[†] [OW...O1[†] 2.709 Å] and F2^{**} [OW...F2^{**} 2.837 Å], respectively, while the hydroxyl group bonds to the F(1^{††}) atom [O(1)...F(1^{††}) 2.765 Å].

Bond valence balance (Table 5) was computed according to Brese and O'Keefe (1991), apart from contribution of the hydrogen, calculated according to Brown and Altermatt (1985). Only small deviations from the exact charge balance were found, for the slightly underbonded F2 and F3, and for the overbonded O1.

Scrutiny of the intensity data shows that the (110) reflection is by far the strongest of all. This is because calcium cations are packed within a structural slab 0.28 Å thick around the (110) plane and F3 anions are located in a 0.54 Å thick slab. The layer of polyhedra parallel to (110) and 4.56 Å thick (Fig. 3), represents

TABLE 5. Bond valence (v.u.) in gearksutite

	F1	F2	F3	F4	O1	OW	Σ_v
Ca	0.30	0.27	0.18	0.25	—	0.17	1.80
			0.23	0.23		0.17	
Al	0.54	0.49	0.48	0.45	0.51	—	2.99
					0.52		
H1	0.12	—	—	—	0.88	—	1.00
HWA	—	—	—	—	0.20	0.80	1.00
HWB	—	0.10	—	—	—	0.90	1.00
Σ_a^v	0.96	0.86	0.89	0.93	2.11	2.04	

a further way of describing the structure. Within this slightly puckered layer the connections between the cations are assured by F2, shared by one Al^{3+} and one Ca^{2+} , F3 and F4, shared by one Al^{3+} and two Ca^{2+} , and OH shared by two Al^{3+} . Each layer is connected to its nearest neighbors only by F1, bridging between one Ca^{2+} and one Al^{3+} , and by one H_2O shared between two Ca^{2+} . Hydrogen bonds too are unevenly distributed among intra- and interlayer connections with respect to these planes. In fact, while one half of water molecules give their hydrogen atoms for interlayer connection with the nearest (110) layers, the other half of water molecules and all the hydroxyl groups are engaged with bond acceptors belonging to the their own layer.

From the above considerations, one could expect that gearksutite crystals would display a platy habit and a good (110) cleavage. The paucity of the material and the small size of the crystals allowed us to perform only a very limited number of tests, in which gearksutite crystals showed an imperfect (110) cleavage, namely parallel to the calcium layers.

The crystal structures of creedite, acuminite and tikhonenkovite also can be conveniently described by means of layers, which have some common features with the (110) layers of gearksutite.

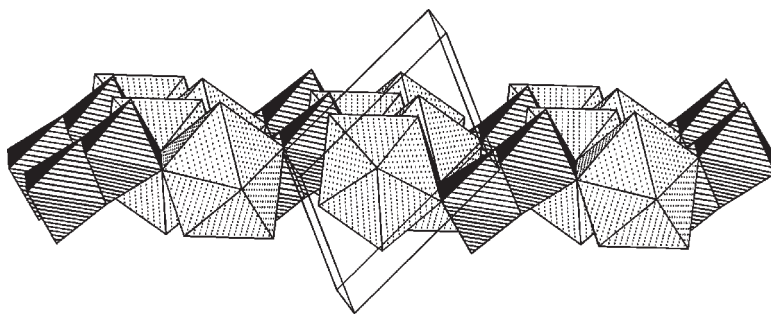


FIGURE 3. Perspective view of the plane 110. The orientation of the unit cell is also shown.

TABLE 6. Calculated and experimental powder patterns of gearksutite from Ivigtut, Greenland

h	k	l	d _{calc}	I _{calc}	Normal Loading		Side Loading	
					d _{obs}	I	d _{obs}	I
0	0	1	6.755	15	6.761	3	6.738	15
0	1	0	6.214	3	—	—	6.206	4
0	1	1	5.233	15	5.232	4	5.223	16
1	1	0	4.575	100	4.575	100	4.567	100
1	1	1	3.808	8	3.810	6	3.804	9
1	1	1	3.769	4	3.771	1	3.771	4
1	0	1	3.530	30	3.533	8	3.528	26
0	0	2	3.377	52	3.379	14	3.376	38
0	1	2	3.316	35	3.317	10	3.313	33
1	2	0	3.171	73	3.170	26	3.167	66
0	2	1	3.117	18	3.120	5	3.117	16
1	2	1	3.022	<1	—	—	3.021	1
1	0	2	2.959	<1	—	—	2.955	2
1	1	2	2.732	15	2.736	2	2.734	4
0	1	2	2.710	11	2.712	2	2.710	10
1	1	1	2.642	16	2.646	3	2.642	14
1	2	2	2.475	5	2.478	1	2.478	4
2	1	0	2.461	2	2.461	2	2.459	1
2	1	1	2.376	4	2.376	2	2.375	3
2	0	0	2.288	50	2.289	19	2.288	42
2	1	1	2.254	22	2.254	7	2.253	19
1	2	0	2.219	13	2.222	4	2.220	13
2	2	1	2.160	38	2.160	19	2.160	37
0	3	1	2.127	5	—	—	2.128	5
1	2	2	2.111	32	2.109	8	2.111	19
1	1	2	2.081	22	2.082	5	2.081	17
0	3	0	2.071	37	2.073	8	2.072	20
1	1	3	2.029	5	2.028	1	2.026	4
1	3	1	2.006	11	2.008	2	2.007	7
0	1	3	1.972	13	1.973	2	1.972	9
2	3	0	1.929	46	1.930	26	1.930	49
1	0	3	1.904	38	1.904	18	1.903	36
1	2	3	1.824	16	1.824	2	1.824	11
2	3	1	1.815	1	1.821	2	1.819	3
2	0	3	1.755	13	1.756	6	1.755	10
0	3	3	1.744	15	—	—	1.745	13
0	1	4	1.739	25	1.739	9	1.738	18
1	4	1	1.700	11	1.702	2	1.701	10
1	3	0	1.671	20	1.673	4	1.672	17
0	2	3	1.648	8	1.648	2	1.648	7
2	3	2	1.616	6	1.615	4	1.615	7
2	1	3	1.604	12	1.599	4	1.599	10
2	2	2	1.585	12	1.586	1	1.585	9
3	2	1	1.563	4	1.565	2	1.565	2
2	1	2	1.540	7	1.542	2	1.540	7
3	3	0	1.525	4	1.526	1	1.526	2
1	0	4	1.506	3	—	—	1.509	3
2	0	3	1.489	7	1.489	1	1.490	9
2	2	1	1.468	5	—	—	1.469	5
1	3	3	1.458	18	1.460	3	1.459	13
3	2	2	1.438	8	1.439	4	1.438	9
3	1	3	1.395	8	1.394	2	1.394	5
3	4	0	1.369	13	1.370	5	1.369	15
3	2	3	1.352	5	1.352	<1	1.351	3
3	3	3	1.269	5	1.269	2	1.268	6
2	4	4	1.237	8	1.238	5	1.239	21
4	2	1	1.229	5	1.227	4	1.227	16
1	2	4	1.206	7	1.207	3	1.207	10
2	3	4	1.187	6	1.187	3	1.187	13
3	2	1	1.143	6	1.142	3	1.142	11
2	6	1	1.126	6	—	—	1.128	3
3	1	5	1.102	6	1.102	1	1.102	6

Note: Where overlapping occurs, the indices of the strongest reflection only are given for the sake of brevity.

In all these phases, the same octahedra pairs $[\text{Al}_2\text{F}_8(\text{OH})_2]$ are linked to eightfold-coordinated Ca^{2+} in creedite and to nine-coordinated Sr^{2+} in the other two phases. Notwithstanding the similarity in chemical composition, the different means of connection between the large-radius cations and the aluminum polyhedra give rise to differently packed layers, markedly puckered in acuminite and tikhonenkovite. However, pairs of adjacent layers are linked in the same way in gearksutite, acuminite and tikhonenkovite, namely by one water molecule and by one fluorine. Structural similarities can also be noticed between gearksutite and the mineral artroite, $\text{PbAlF}_3(\text{OH})_2$, (Kampf and Foord 1995) in which the crystal structure consists of structural layers, parallel to (101), built up by $[\text{Al}_2\text{F}_6(\text{OH})_4]$ linked to nine-coordinated lead cations. As in gearksutite, these layers are only slightly puckered and all the Al_2X_{10} pairs are is oriented.

Both in gearksutite and artroite, the presence of slightly puckered structural layers correlates with the presence, in the powder pattern of the two minerals, of a very strong reflection with the same indices as the structural layers. This is not true for acuminite and tikhonenkovite, where markedly puckered layers are present.

X-RAY POWDER PATTERN OF GEARKSUTITE

X-ray powder data (Table 6) were collected on a Philips PW1050 diffractometer, using 0.02° 2θ steps from 4 to 90° and counting 15 s per step, using samples coming from three different localities: Ivigtut (type locality), Chancellor mine, Colorado, and Vulcano island, Italy. The three patterns were not significantly different.

Indexing of the pattern was performed taking into account the single crystal intensity data set through the XPOW program, a part of the SHELXTL suite (Sheldrick 1992).

The above structural considerations together with the intensities calculated from single crystal data, suggested that the experimental patterns may be affected by strong (110) preferred orientation. This was confirmed by comparing the powder patterns obtained with the normal and side loaded mount. The effectiveness of side loading in randomizing the powder orientation was tested by Rietveld refinement of both the collected patterns.

The refinement was performed with the GSAS program (Larson and Von Dreele 1988). Together with background, scale factor, lattice parameters, and three profile coefficients in the 18 term pseudo-Voigt function, the preferred orientation was modeled following the formulation of Dollase (1986). The preferred orientation refinement coefficient converged to 0.742 for the

normal data collection (final reliability factor $R = 0.126$) and to 0.963 for the side loading collection (final $R = 0.098$).

ACKNOWLEDGMENTS

W.D. Birch of Museum of Victoria, Australia, is gratefully acknowledged for having provided us with gearksutite specimens (registration number M38124). S. Merlino of Pisa University is thankfully acknowledged for helpful discussion. The Ministero dell'Università e della Ricerca Scientifica e Tecnologica, MURST, is acknowledged for financial support.

REFERENCES CITED

- Bernauer, F. (1941) Eine Gearksutite-Lägerstätte auf der Insel Vulcano. *Zeitschrift der Deutschen Geologischen Gesellschaft*, 93 (10), 65–80
- Birch, W.D. and Pring, A. (1990) A calcian ralstonite-like mineral from the Cleveland Mine, Tasmania, Australia. *Mineralogical Magazine*, 54, 599–602.
- Boscardin, M., Marchetti, F., Orlandi, P., and Zordan, A. (1995) La gearksutite della Valle dei Mercanti (Torrebelvicino, Vicenza). *Atti della Società Toscana di Scienze Naturali, Serie A*, 102, 117–120.
- Breese, N.E. and O'Keeffe, M. (1991) Bond-valence parameters for solids. *Acta Crystallographica*, B47, 192–197.
- Brown, I.D. and Altermatt, D. (1985) Bond valence parameters obtained from a systematic analysis of the inorganic structure database. *Acta Crystallographica*, B41, 244–247.
- Dollase, W.A. (1986) Correction of intensities for preferred orientation in powder diffractometry: Application of the March model. *Journal of Applied Crystallography*, 19, 267–272.
- Giacovazzo, C. and Marchetti, S. (1969) The crystal structure of prosopite. *Atti dell'Accademia Nazionale dei Lincei, Classe di Scienze Fisiche, Matematiche e Naturali, Rendiconti*, 47, 55–68.
- Giuseppetti, G. and Tadini, C. (1983) Structural analysis and refinement of Bolivian creedite, $\text{Ca}_3\text{Al}_2\text{F}_8(\text{OH})_2(\text{SO}_4) \cdot 2\text{H}_2\text{O}$. The role of the hydrogen atoms. *Neues Jahrbuch für Mineralogie Monatshefte*, 2, 69–78.
- Hagemann, G. in Dana, J.D. (1868) *A system of Mineralogy*, fifth edition. J. Wiley & Sons, New York.
- Hawthorne, F.C. (1984) The crystal structure of stenonite and the classification of the aluminofluoride minerals. *Canadian Mineralogist*, 22, 245–251.
- Kampf, A.R. and Ford, E.E. (1995) Artroeite, $\text{PbAlF}_3(\text{OH})_2$, a new mineral from the Grand Reef mine, Graham County, Arizona: Description and crystal structure. *American Mineralogist*, 80, 179–183.
- Krogh Andersen, E. and Ploug-Sørensen, G. (1991) The structure of acuminite, a strontium aluminum fluoride mineral. *Zeitschrift für Kristallographie*, 194, 221–227.
- Larson, A.C. and Von Dreele, R.B. (1988) *Generalized Structure Analysis System*. Los Alamos National Laboratory report, LAUR 86–748, 150 p.
- Muetterties, E.L. and Guggenberger, L.J. (1973) Idealized polytopal forms. Description of real molecules referenced to idealized polygons or polyhedra in geometric reaction path form. *Journal of the American Chemical Society*, 96, 1748–1756.
- Pudovkina, Z.V. and Pyatenko, Yu.A. (1967) Crystal structure of tikhonenkovite, $\text{Sr}_2[\text{Al}_2\text{F}_8(\text{OH})_2] \cdot 2\text{H}_2\text{O}$. *Doklady Akademii Nauk SSSR, Earth Sciences Section*, 174, 117–120.
- Raade, G. and Haug, J. (1980) Rare fluorides from a soda granite in the Oslo region, Norway. *Mineralogical Record*, 11, 83–91.
- Sheldrick, G.M. (1992) *SHELXTL, Release 5.03*. Siemens Analytical X-ray Instruments Inc., Madison, Wisconsin, U.S.A.

MANUSCRIPT RECEIVED NOVEMBER 9, 1998

MANUSCRIPT ACCEPTED AUGUST 11, 1999

PAPER HANDLED BY JAMES W. DOWNS